



# Why the oxygen IR emission at 1.27 $\mu\text{m}$ is not the best method for ozone retrieval in the mesosphere?

Rada O. Manuilova, [r.manuylova@spbu.ru](mailto:r.manuylova@spbu.ru), Valentine A. Yankovsky\*, [vyankovsky@gmail.com](mailto:vyankovsky@gmail.com),  
Saint-Petersburg State University, Department of Atmospheric Physics



YM-2011 - model of electronic vibrational kinetics of excited products of  $\text{O}_3$  and  $\text{O}_2$

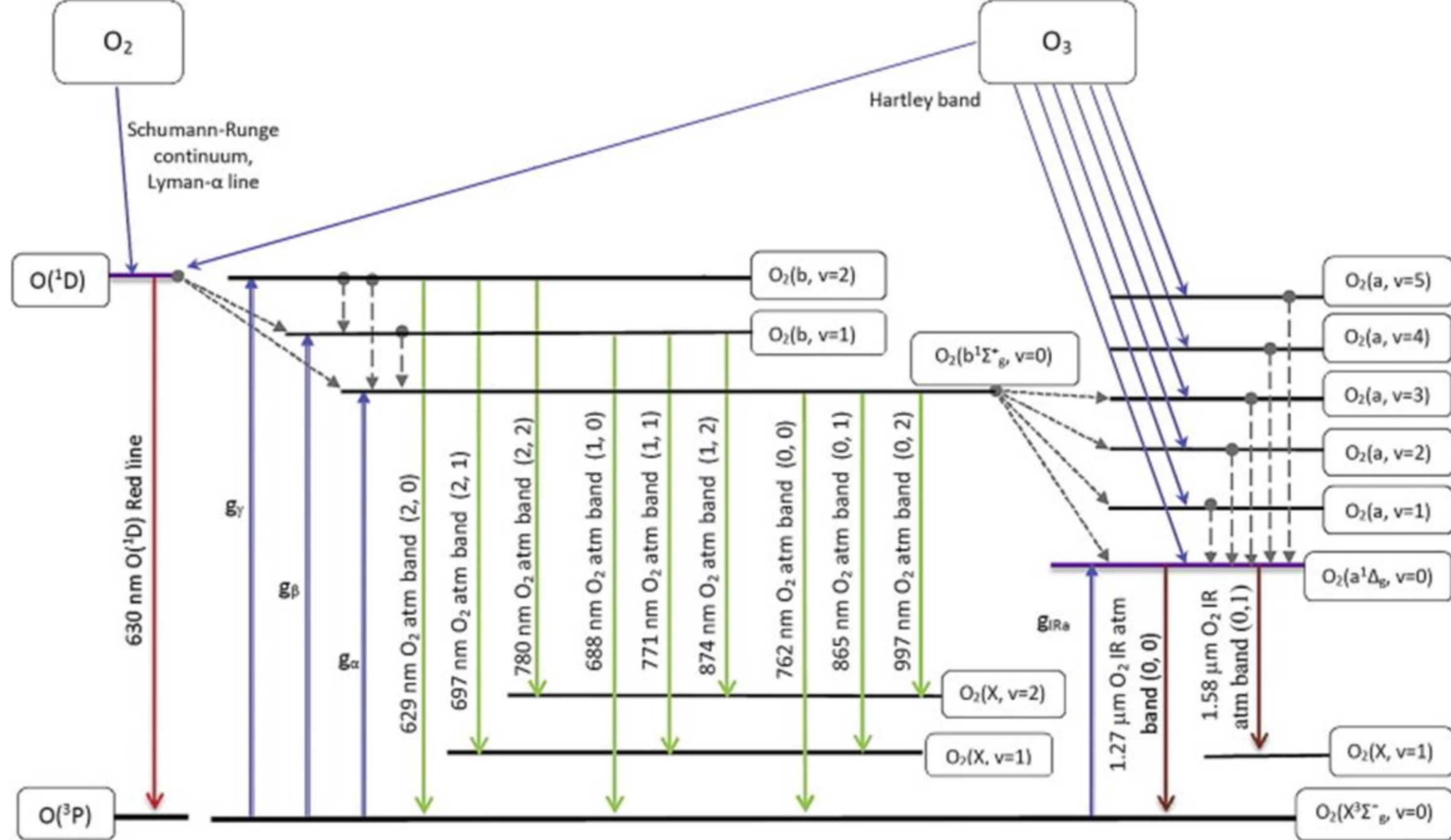


Fig.1. The model takes into account 10 excited states of molecules of oxygen  $\text{O}_2(\text{b}^1\Sigma_g^-, v=0-2)$ ,  $\text{O}_2(\text{a}^1\Delta_g, v=0-5)$  and metastable atom  $\text{O}(\text{1D})$  and more than 60 aeronomical reactions.

Sloping lines – the processes of  $\text{O}_2$  and  $\text{O}_3$  photolysis. Double vertical lines – the processes of solar radiation absorption in the 762 nm ( $g_{\alpha}$ ), 688 nm ( $g_{\beta}$ ), 629 nm ( $g_{\gamma}$ ) and in the 1.27  $\mu\text{m}$  ( $g_{\text{IRa}}$ ) bands. Slant lines – energy transfer from  $\text{O}(\text{1D})$  to the  $\text{O}_2(\text{b}^1\Sigma_g^-, v=0, 1)$  and from  $\text{O}_2(\text{b}^1\Sigma_g^-, v=0)$  to  $\text{O}_2(\text{a}^1\Delta_g, v=0-3)$  and from  $\text{O}_2(\text{b}^1\Sigma_g^-, v)$  at collisional quenching. Dashed lines – the processes of V-V and V-T relaxation. Red line – the processes of radiative emissions from  $\text{O}(\text{1D})$  (630 nm). Green lines – the processes of radiative emissions from electronic-vibrational levels  $\text{O}_2(\text{b}^1\Sigma_g^-, v=0-2)$ . Brown lines – processes of radiative emissions from  $\text{O}_2(\text{a}^1\Delta_g, v=0)$  to  $\text{O}_2(\text{X}^3\Sigma_g^-, v=0, 1)$ . All emissions could be used as proxies of  $[\text{O}_3]$  and  $[\text{O}(\text{3P})]$  in MLT.

## Problems

In the framework of model of electronic vibrational kinetics of excited products of  $\text{O}_3$  and  $\text{O}_2$  photolysis in the MLT of the Earth, YM2011, we have tried to answer the formulated above question. In our study we propose to retrieve the  $[\text{O}_3]$  using as proxies electronic-vibrationally excited levels of oxygen molecule, namely  $\text{O}_2(\text{b}^1\Sigma_g^-, v=0, 1)$ ,  $\text{O}_2(\text{a}^1\Delta_g, v=0)$  and excited atom  $\text{O}(\text{1D})$  (Fig. 1). Population of  $\text{O}_2(\text{b}^1\Sigma_g^-, v=2)$  doesn't depend on  $[\text{O}_3]$  (Fig. 2). Concerning the  $[\text{O}_3]$  retrieval in the range of 50–100 km, the emission at 1.27  $\mu\text{m}$  formed by transition from  $\text{O}_2(\text{a}^1\Delta_g, v=0)$  and emission at 762 nm formed by transition from  $\text{O}_2(\text{b}^1\Sigma_g^-, v=0)$  are the most intensive ones among all emissions under consideration. However, considering the complexity of kinetics of the excited components: choosing  $\text{O}(\text{1D})$  as a proxy for  $[\text{O}_3]$  retrieval, requires taking into account five aeronomical reactions. For other proxies the number of aeronomical reactions is as follows:  $\text{O}_2(\text{b}^1\Sigma_g^-, v=1) - 13$ ;  $\text{O}_2(\text{b}^1\Sigma_g^-, v=0) - 18$ ;  $\text{O}_2(\text{a}^1\Delta_g, v=0) - 25$ . Increasing the number of reactions that must be considered when using a proxy from  $\text{O}(\text{1D})$  to  $\text{O}_2(\text{a}^1\Delta_g, v=0)$  depends on the fact that, calculating the population of each of the underlying electronic-vibrationally excited state requires considering the mechanisms of the population of the upper levels. Using the  $\text{O}_2(\text{a}^1\Delta_g, v=0)$  is also associated with the problem of poorly known rate coefficients for some important processes. For example, the rate constant of reaction  $\text{O}_2(\text{a}^1\Delta_g, v=0) + \text{O}(\text{3P}) \rightarrow \text{products}$  is known with uncertainty 200%,  $\text{O}_2(\text{b}^1\Sigma_g^-, v=0) + \text{O}(\text{3P}) \rightarrow \text{products}$  (with uncertainty 25 – 300%),  $\text{O}_2(\text{a}^1\Delta_g, v \geq 1) + \text{O}_3 \rightarrow \text{products}$  (with uncertainty 43%) etc.

## Results of sensitivity study

The next criterion of a “good” proxy is the value of  $[\text{O}_3]$  retrieval uncertainty. Above 90 km,  $\text{O}_2(\text{a}^1\Delta_g, v=0)$  becomes the worst proxy among all under consideration with the uncertainty exceeding 100% (Fig. 3b). In the interval 50–98 km  $\text{O}_2(\text{b}^1\Sigma_g^-, v=1)$  is the “good” proxy with the value of uncertainty less than 20% below 90 km and less than 25% up to 98 km (Fig. 3a). Therefore,  $\text{O}_2(\text{b}^1\Sigma_g^-, v=1)$  is the preferable proxy at the altitudes of 50–98 km. Commonly used  $[\text{O}_3]$  retrieval proxy,  $\text{O}_2(\text{a}^1\Delta_g, v=0)$ , transition from which forms the 1.27  $\mu\text{m}$   $\text{O}_2$  IR Atmospheric band, has more than one hour photochemical lifetime in the MLT. On the other hand, the  $\text{O}(\text{1D})$  and  $\text{O}_2(\text{b}^1\Sigma_g^-, v=0, 1)$  lifetime in the altitude region of 50–200 km is less than 14 sec (Fig. 4). So, the proposed  $\text{O}_2(\text{b}^1\Sigma_g^-, v=0, 1)$  and  $\text{O}(\text{1D})$  proxies can be used for tracking fast variations of the  $\text{O}_3$  atmospheric concentrations generated by wave processes, electron precipitations, solar flux changes, and so on, when the  $\text{O}_2(\text{a}^1\Delta_g, v=0)$  proxy becomes useless.

## The more suitable alternatives exist!

Based on this complex analysis we concluded that the optimal proxy for  $[\text{O}_3]$  retrieval is  $\text{O}_2(\text{b}^1\Sigma_g^-, v=1)$  in the altitude interval 50–98 km and  $\text{O}_2(\text{b}^1\Sigma_g^-, v=0)$  in the altitude interval 85–98 km. It should be noted, that lifetimes of  $\text{O}_2(\text{b}^1\Sigma_g^-, v=0, 1)$  and 2) are not more than 14 sec in MLT, what gave the opportunity to register the short-period  $[\text{O}(\text{3P})]$  and  $[\text{O}_3]$  variations. It is important to note that above 100 km neither of the proxies under consideration can provide ozone retrieval of sufficient accuracy.

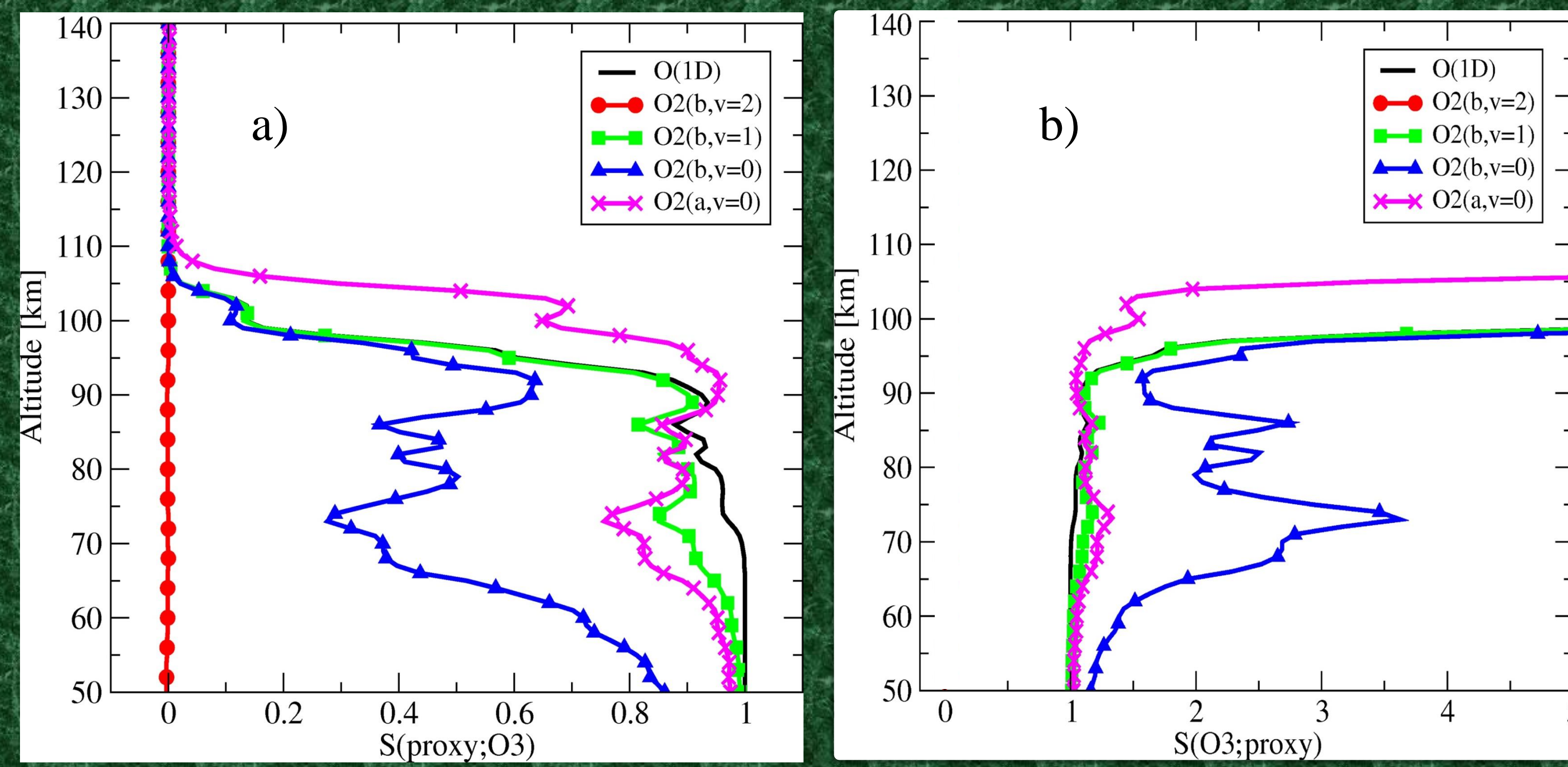


Fig.2. a) Sensitivity coefficient of the proxy concentration to  $[\text{O}_3]$  for the forward problem,  $S(\text{proxy}; \text{O}_3)$ . b) Sensitivity coefficient of  $[\text{O}_3]$  to the proxy concentration for the inverse problem,  $S(\text{O}_3; \text{proxy})$ . Type of proxy:  $\text{O}(\text{1D})$  – black line;  $\text{O}_2(\text{b}^1\Sigma_g^-, v=2)$  – red line with filled circles;  $\text{O}_2(\text{b}^1\Sigma_g^-, v=1)$  – green line with filled squares;  $\text{O}_2(\text{b}^1\Sigma_g^-, v=0)$  – blue line with filled triangles;  $\text{O}_2(\text{a}^1\Delta_g, v=0)$  – rose line with crosses. Optimal proxies for  $[\text{O}_3]$  retrieval are:  $\text{O}_2(\text{b}^1\Sigma_g^-, v=1)$ ,  $\text{O}_2(\text{a}^1\Delta_g, v=0)$  and  $\text{O}(\text{1D})$ .

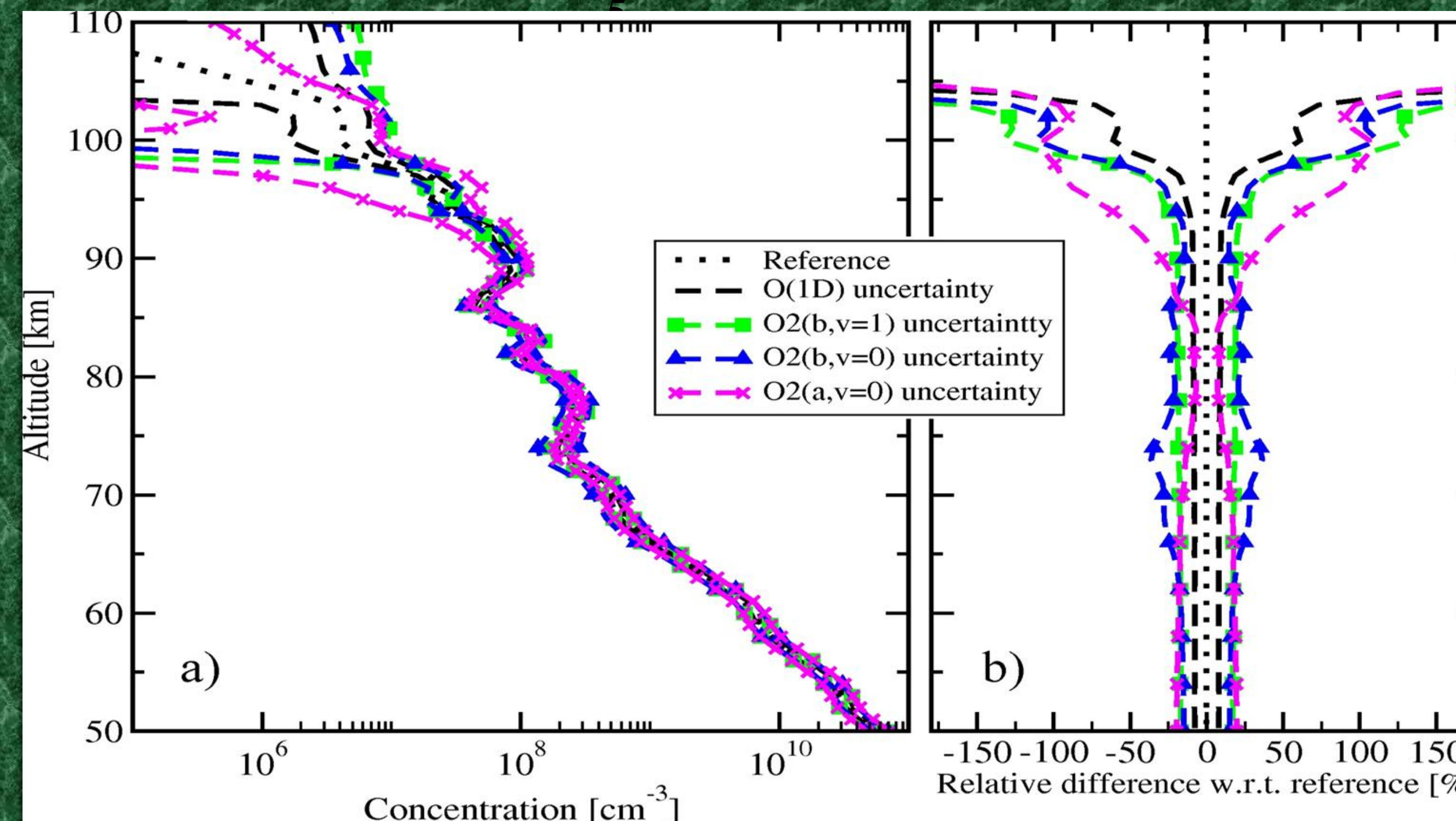


Fig 3. Uncertainties of  $[\text{O}_3]$  retrieval (the limits  $\pm\sigma$ ) for different proxies:

a) absolute values, b) relative values.

The predetermined reference altitude profile of  $[\text{O}_3]$  is presented by the dotted curve, and is taken from SABER L2,2010, day 172, latitude 43.0,  $\text{SZA}=70.5$ . Type of proxy:  $\text{O}(\text{1D})$  – black dashed line;  $\text{O}_2(\text{b}^1\Sigma_g^-, v=1)$  – green dashed line with filled squares;  $\text{O}_2(\text{b}^1\Sigma_g^-, v=0)$  – blue dashed line with filled triangles;  $\text{O}_2(\text{a}^1\Delta_g, v=0)$  – rose dashed line with crosses.

## Comments to Figures 2 and 3.

In the range of 50–85 km,  $\text{O}_2(\text{a}^1\Delta_g, v=0)$  is available proxy, with an uncertainty value of less than 15 – 20%. Above 90 km,  $\text{O}_2(\text{a}^1\Delta_g, v=0)$  becomes the worst proxy, with uncertainty exceeding 100% (rose curve in Fig. 3). In terms of the ‘worst’ proxy in the mesosphere (up to 90 km),  $\text{O}_2(\text{b}^1\Sigma_g^-, v=0)$ , the value of retrieval uncertainty exceeds 35% at 65-80 km (blue curve in Fig. 3).

Therefore,  $\text{O}_2(\text{b}^1\Sigma_g^-, v=1)$  is the preferable proxy at altitudes of 50–98 km (green curve in Fig. 3). It is important to note that, according to Fig. 2 and Fig. 3, at above 98 km neither of the proxies under consideration can provide ozone retrieval of sufficient accuracy.

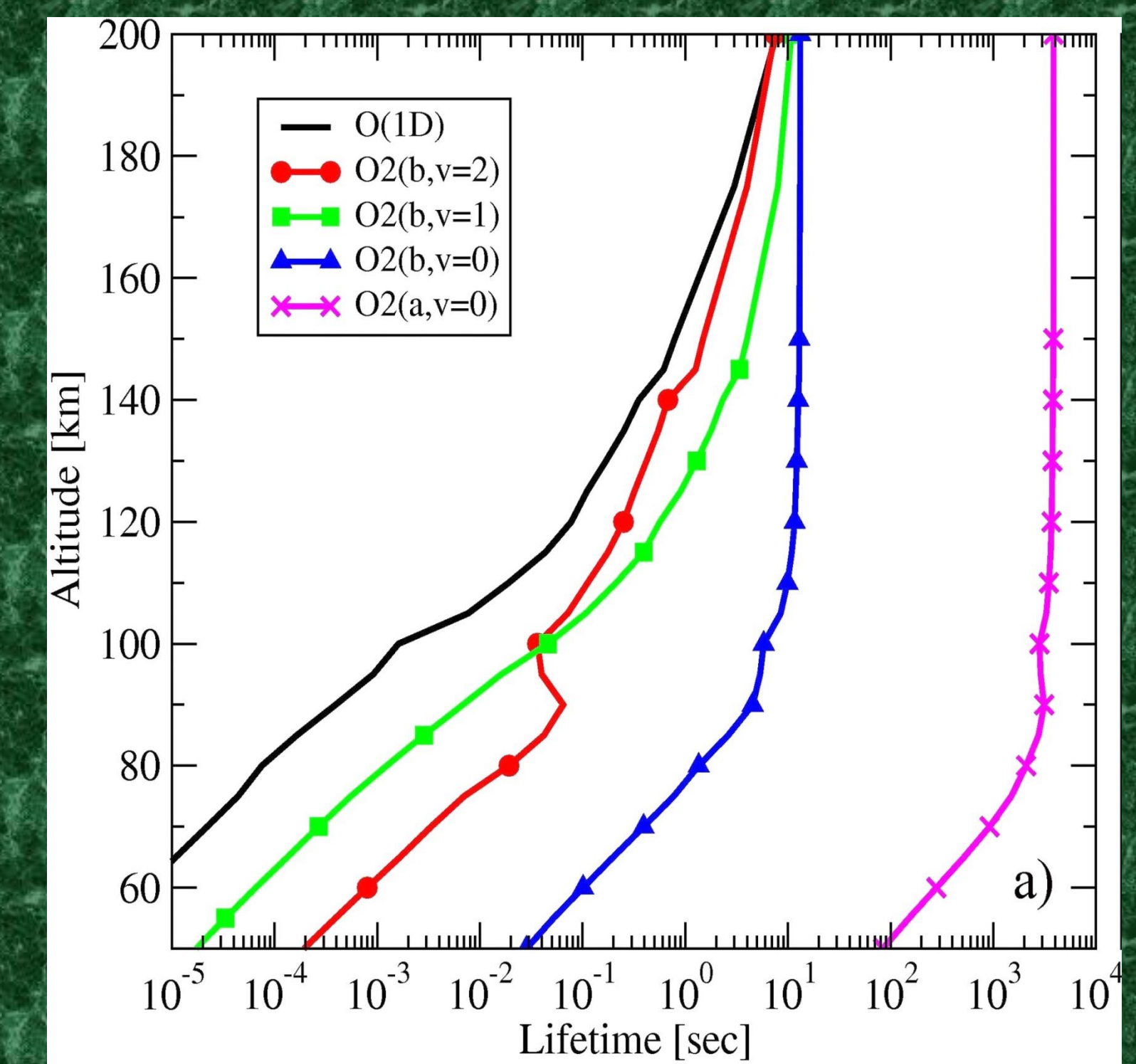


Fig 4. Typical photochemical lifetimes of proxies  $\text{O}(\text{1D})$ ,  $[\text{O}_2(\text{b}^1\Sigma_g^-, v=0, 1, 2)]$  and  $\text{O}_2(\text{a}^1\Delta_g, v=0)$  in the mesosphere and lower thermosphere. See the type of proxy in the caption to Fig. 2.

Note:  $\text{O}_2(\text{a}^1\Delta_g, v=0)$  lifetime is about one hour, the lifetimes of the other proxies are less than 14 sec.